Dynamic process of the resonant phonon scattering in fully filled skutterudites

Yancheng Wang,[1,2] Hongliang Yang,[1,2,3] Wujie Qiu,[1] Jiong Yang,[4,*] Jihui Yang,[5] and Wenqing Zhang[3,1,*]

[1]*State Key Laboratory of High Performance Ceramics and Superfine Microstructure, Shanghai Institute of Ceramics, Chinese Academy of Sciences, Shanghai 200050, China*

[2]*University of Chinese Academy of Sciences, Beijing 100049, China*

[3]*Department of Physics and Shenzhen Institute for Quantum Science & Technology, Southern University of Science and Technology, Shenzhen 518055, China*

[4]*Materials Genome Institute, Shanghai University, Shanghai 200444, China*

[5]*Materials Science and Engineering Department, University of Washington, Seattle, Washington 98195, USA*

(Received 9 April 2018; published 9 August 2018)

The dynamics of the phonon scattering caused by the guest-host interactions in fully filled skutterudites (Yb, La, Ba)Fe_4Sb_{12} are studied by *ab initio* molecular dynamics. The characteristics of filler vibrations are found to be the origin of ultralow lifetimes for the filler-dominant modes. Under the phonon-phonon interaction diagram, the large amplitudes of the filler vibrations and the coupling between filler and framework phonon modes greatly increase the strength of phonon scatterings. The lattice thermal conductivities for the three skutterudites, however, are all overestimated comparing with the experimental results. The introduction of the resonant scattering is thus necessary to account for the deviations. Furthermore, by applying the wavelet-based analysis to the resonant scattering process, the time-frequency power spectrum shows clearly that the time-varying localized motions of the fillers periodically absorb the heat-carrying lattice phonons and emit them. This process is the origin of the resonant scattering mechanism in skutterudites, and strongly interferes with the propagation of phonons near the frequency range of the fillers.

DOI: 10.1103/PhysRevB.98.054304

I. INTRODUCTION

Many important measurable properties of materials are related with their lattice dynamics and phonon interactions. In thermoelectric materials, lattice thermal conductivity (κ_L) is crucial for a high thermoelectric figure of merit. Filled skutterudites are typical examples of "phonon glass" materials with low κ_L since their oversized icosahedral cages can be filled by heavy atoms [1–3]. The loose bonding nature between the guest atom and the host framework causes a localized vibration of the fillers [4], resulting in a considerable amount of scattering of the low-frequency propagative phonons. Under the guidance of this paradigm, multiple-filled skutterudites achieve broad-frequency phonon scattering and greatly suppressed κ_L [5]. However, how the localized nature of the filler vibration affects the thermal transport in filled skutterudites is still in debate.

The generally accepted explanation is the phenomenological theory of the resonant phonon scattering mechanism which has been used to fit measured low thermal conductivities in experiments. The nondispersive and intense peak in partial phonon density of states (PDOS) measured by inelastic neutron scattering (INS) implies the harmonic and localized trait of the filler vibration [6]. The heat capacity measurements treat the filler vibration modes as independent and localized Einstein oscillators [7–9]. Besides, the avoided crossing behaviors in both skutterudites [10] and clathrates [11] demonstrate a harmonic coupling between the fillers and the frameworks [12]. Although these experimental and theoretical evidences support the argument of resonant scattering, the microscopic process about how the filler interacts with the framework and scatters the acoustic phonons is still ambiguous.

The alternative explanation of fillers on lowing κ_L is the enhanced three-phonon scattering channels due to the flattened optical phonon branches caused by the presence of filler atoms [10,13], supported by the phase coherence inferred from INS studies in (La, Ce)Fe_4Sb_{12} [13]. However, INS measurements on the analogous guest-host system–clathrate compounds [11,14] show that the broadening of the acoustic phonon peak is not enough to explain the reduced κ_L. Besides, the calculated κ_L of $YbFe_4Sb_{12}$ [15], carried out by the standard lattice dynamics calculations, is significantly lower than the reported experimental data [16].

Our recent work [17] has given a more reasonable calculated κ_L of $YbFe_4Sb_{12}$, which is higher than the measured one by 50%. This result demonstrates that the theoretical lattice dynamics of this compound could be very different if considering the finite-temperature phonon-phonon interactions evaluated by the *ab initio* molecular dynamics (AIMD) simulation, as well as the temperature-dependent effective potential (TDEP) approach [18,19]. Due to the overestimation of the κ_L, the phenomenological resonant scattering is necessary to make the theoretical κ_L more agreeable with the experiment. It is thus interesting to validate the generality of introducing the resonant scattering in this series of compounds. More importantly, the physical origin of this mechanism ought to be explored.

In this paper, we will demonstrate the dynamic process of filler vibrations, and their relationship with the resonant

*Corresponding authors: jiongy@t.shu.edu.cn and zhangwq@sustc.edu.cn

scattering in filled skutterudites. The paper is organized as follows. First, we examine the phonon transport properties of three fully filled skutterudites, (Yb, La, Ba)Fe_4Sb_{12} under the perturbation theory, considering the phonon-phonon interactions at finite temperatures. The detailed analysis shows that the quasilocalized nature of filler vibration modes causes strong phonon scattering and reduced phonon relaxation time; the κ_Ls, however, are still overestimated. Then, the time-frequency features of the filler trajectories are investigated by adopting the wavelet analysis on the velocity correlation functions. The results suggest that some lattice phonons will be absorbed and emitted periodically in the time-varying process of filler vibration frequencies. This dynamic process strongly inhibited the propagation of phonons at the vicinity of the frequency ranges of the fillers, giving rise to the resonant scattering.

II. METHOD

Given the large-amplitude vibrations of fillers, their potential energy surfaces obtained by the frozen phonon method [15] become questionable. Therefore, we carry out the AIMD simulations of (Yb, La, Ba)Fe_4Sb_{12} at 300–600 K. In order to account for the lattice expansion, lattice parameters at these temperatures are estimated by the quasiharmonic approximation (QHA) carried out by the PHONOPY package [20], and adopted for the AIMD simulations. The AIMD calculations are carried out by the VASP code [21], with the PAW method [22] and the Perdew-Burke-Ernzerhof functional [23]. More details of the computation are listed in the Supplemental Material [24]. The temperature-dependent harmonic and anharmonic interatomic force constants (IFCs) are extracted from the trajectories and forces of AIMD by the TDEP method [18,19]. The strength of three-phonon interactions $\Phi_{\lambda\lambda'\lambda''}$ can be gotten by

$$\boldsymbol{\Phi}_{\lambda\lambda'\lambda''} = \sum_{ijk}\sum_{\alpha\beta\gamma} \frac{\boldsymbol{e}^{\lambda}_{\alpha i}\boldsymbol{e}^{\lambda'}_{\beta j}\boldsymbol{e}^{\lambda''}_{\gamma k}}{\sqrt{\boldsymbol{M}_i\boldsymbol{M}_j\boldsymbol{M}_k}\sqrt{\boldsymbol{\omega}_{\lambda}\boldsymbol{\omega}_{\lambda'}\boldsymbol{\omega}_{\lambda''}}}\boldsymbol{\Phi}^{\alpha\beta\gamma}_{ijk} \times \boldsymbol{e}^{i(\boldsymbol{q}\boldsymbol{r}_i+\boldsymbol{q}'\boldsymbol{r}_j+\boldsymbol{q}''\boldsymbol{r}_k)}\Delta(\boldsymbol{q}+\boldsymbol{q}'+\boldsymbol{q}''), \quad (1)$$

where $\Phi^{\alpha\beta\gamma}_{ijk}$ is the element of the anharmonic IFC tensor, and ijk are the atom indices; α indicates the Cartesian directions in the real space. λ is the phonon mode of the branch s at the wave vector $\boldsymbol{q}$. $e^{\lambda}_{\alpha i}$ is the eigenvector for atom i along the αth direction in the λ mode. M_i is the mass of atom i. $\Delta(\boldsymbol{q}+\boldsymbol{q}'+\boldsymbol{q}'')$ represents the quasiconservation of the momentum. According to the Fermi golden rule in the perturbation theory, the linewidth of the phonon mode [25] can be obtained as

$$\boldsymbol{\Gamma}_{\lambda}(\boldsymbol{\omega}) = \frac{\hbar\boldsymbol{\pi}}{16}\sum_{\lambda'\lambda''}|\boldsymbol{\Phi}_{\lambda\lambda'\lambda''}|^2[(\boldsymbol{n}_{\lambda'}+\boldsymbol{n}_{\lambda''}+1)\boldsymbol{\delta}(\boldsymbol{\omega}-\boldsymbol{\omega}_{\lambda'}-\boldsymbol{\omega}_{\lambda''}) + 2(\boldsymbol{n}_{\lambda'}-\boldsymbol{n}_{\lambda''})\boldsymbol{\delta}(\boldsymbol{\omega}-\boldsymbol{\omega}_{\lambda'}+\boldsymbol{\omega}_{\lambda''})], \quad (2)$$

where n_λ is the occupation number of the λ mode satisfying the Bose-Einstein distribution. The joint densities of states (JDOS), known as three-phonon scattering channels, are also estimated as

$$\boldsymbol{D}^{\pm}(\boldsymbol{q},\boldsymbol{\omega}) = \frac{1}{\boldsymbol{N}}\sum_{\lambda'\lambda''}\boldsymbol{\delta}(\boldsymbol{\omega}\pm\boldsymbol{\omega}_{\lambda'}-\boldsymbol{\omega}_{\lambda''}) \times\Delta(\boldsymbol{q}+\boldsymbol{q}'+\boldsymbol{q}''), \quad (3)$$

where the + (–) indicates the absorption (emission) process. Then the phonon lifetimes would be obtained as $\tau_\lambda(\omega) = 1/2\Gamma_\lambda(\omega)$. The lattice thermal conductivity is calculated in the relaxation time approximation (RTA) as

$$\boldsymbol{\kappa}_{\boldsymbol{L}} = \frac{1}{\boldsymbol{NV}}\sum_{\lambda}\boldsymbol{C}_{\lambda}\boldsymbol{v}^2_{\lambda}\boldsymbol{\tau}_{\lambda}. \quad (4)$$

Apart from those methods on the finite-temperature lattice dynamics mentioned above, we also employ velocity correlation functions to analyze the dynamic characteristics of filler vibrations. The regular approach is applying the Fourier transform on the velocity autocorrelation function (VAF) or cross correlation function (VCF) to get the power spectra information in the frequency domain [26]. The result is rather a statistical average over the long time scale. Here, we are going to characterize the variation of the filler vibrations and to elucidate their influences on the phonon transport. In order to achieve this goal, we make the wavelet transform instead on the VAF of those fillers, and attain their vibration energy on the time-frequency plane [27,28], as described by

$$\boldsymbol{W}_i(\boldsymbol{n},\boldsymbol{s}) = \int_{-\infty}^{+\infty}\langle\boldsymbol{v}_i(0)\boldsymbol{v}_i(\boldsymbol{t})\rangle\boldsymbol{\Psi}\left(\frac{\boldsymbol{t}-\boldsymbol{n}\boldsymbol{\delta}\boldsymbol{t}}{\boldsymbol{s}}\right)\boldsymbol{dt}, \quad (5)$$

where $\Psi(\frac{t-n\delta t}{s})$ is the wavelet basis. To better reproduce the power spectra, we choose the Morlet wavelet as the basis function, which is actually a cosine function with a Gaussian envelope shown by

$$\Psi(\boldsymbol{t}) = \boldsymbol{\pi}^{-1/4}\cos(5\boldsymbol{t})\boldsymbol{e}^{-\boldsymbol{t}^2/2}. \quad (6)$$

Equation (6) shows that n shifts the wavelet along the time axis and s stretches the time window scale of the wavelet, the reciprocal of which is the frequency ω (see the Supplemental Material [24]). That is why the wavelet analysis could obtain the time-frequency spectrum. In the Supplemental Material [24], simple examples of gas and liquid atoms motions [29] are given to illustrate the role of wavelet analysis on determining the dynamic process.

Moreover, we do the same thing on the VCF $\langle\boldsymbol{v}_i(0)\boldsymbol{v}_j(t)\rangle$ between the filler and the neighboring framework, and get their cross correlation spectrum $s_{ij}(t,\omega)$ [30]. When normalized by the power spectra, it turns out to be the time-frequency coherence $C_{ij}(t,\omega)$, a dimensionless value within the interval [0, 1], as shown by

$$\boldsymbol{C}_{ij}(\boldsymbol{t},\boldsymbol{\omega}) = \frac{|\boldsymbol{s}_{ij}(\boldsymbol{t},\boldsymbol{\omega})|^2}{\boldsymbol{s}_{ii}(\boldsymbol{t},\boldsymbol{\omega})\boldsymbol{s}_{jj}(\boldsymbol{t},\boldsymbol{\omega})}. \quad (7)$$

If $\boldsymbol{v}_i(t)$ and $\boldsymbol{v}_j(t)$ are totally correlated or linearly dependent, it is certainly that $C_{ij} \approx 1.0$. Conversely, two random atomic motions would make C_{ij} approach zero. Thus, we are able to measure the dynamic correlation properties between fillers and framework and to figure out the relationship between the guest-host interactions and the resonant scattering.

III. RESULTS AND DISCUSSION

A. Finite-temperature three phonon interaction

We first examine the vibration features of fillers in the room-temperature lattice dynamics of these three filled skutterudites. The participation ratio (PR) [14,31] is usually adopted to

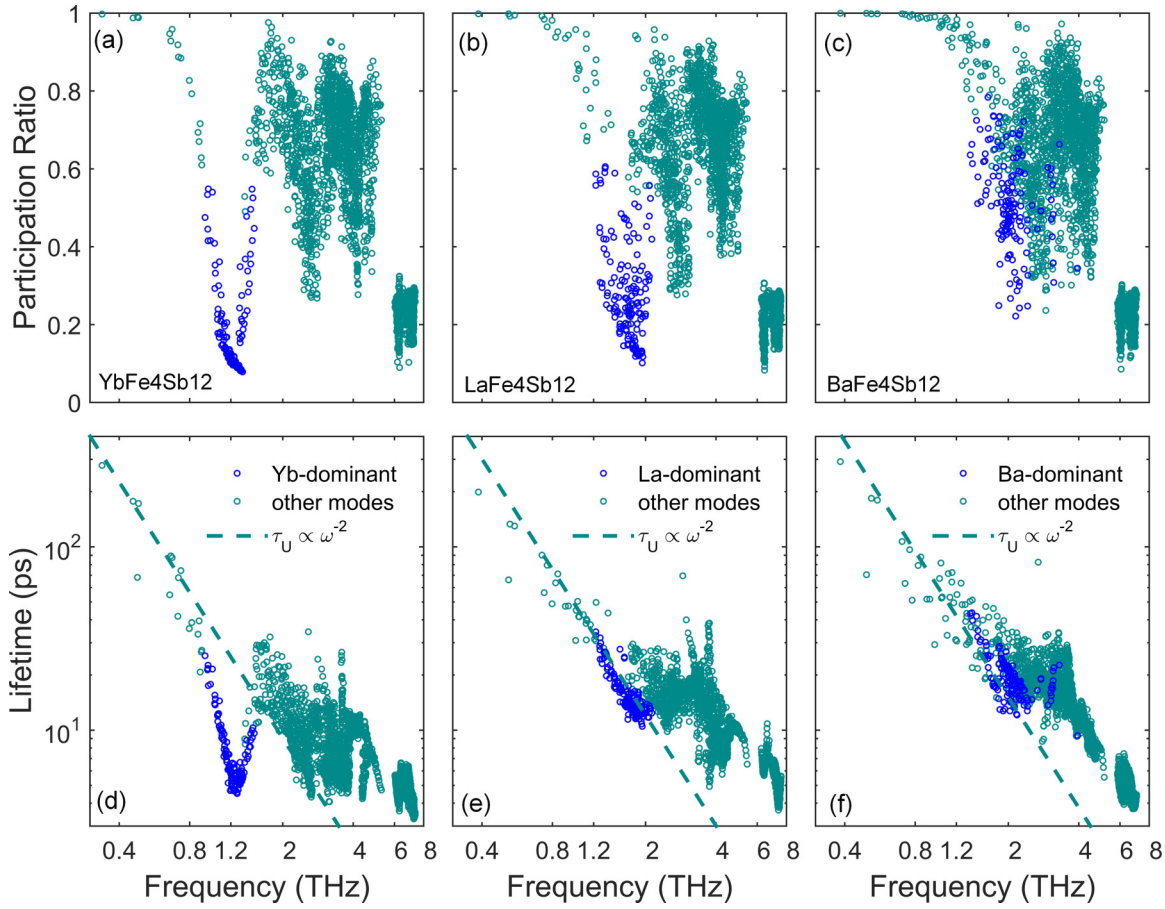

FIG. 1. Calculated participation ratio (top) and phonon lifetimes (down) versus frequencies of filled skutterudites, $YbFe_4Sb_{12}$ [17] (a,d), $LaFe_4Sb_{12}$ (b,e), and $BaFe_4Sb_{12}$ (c,f), at 300 K. Phonon lifetimes of framework-dominant modes are fitted by $\tau_U \propto \omega^{-2}$ as a comparison.

characterize the localization of the phonon mode by the participation degree of all atoms as described by

$$p(\boldsymbol{\omega}_\lambda) = \left[\sum_i^N \left|\frac{\boldsymbol{e}_i(\boldsymbol{\omega}_\lambda)}{\sqrt{\boldsymbol{M}_i}}\right|^2\right]^2 \Big/ N\sum_i^N \left|\frac{\boldsymbol{e}_i(\boldsymbol{\omega}_\lambda)}{\sqrt{\boldsymbol{M}_i}}\right|^4, \quad (8)$$

where $\boldsymbol{e}_i(\omega_\lambda)/\sqrt{M_i}$ is the displacement amplitudes of the atom i. The PR closing to 1.0 means the propagative phonon modes, like the acoustic branches; the PR around or lower than 0.2 indicates the localized mode where very few atoms have large displacements and other atoms keep still [31]. As shown in Fig. 1(a), Yb-dominant modes are localized since their PR is mainly concentrated on the part lower than 0.2. The La vibration [Fig. 1(b)] becomes quasilocalized with PR mainly distributed in the range from 0.1 to 0.4. The Ba-dominant modes are entangling with vibrations of framework atoms implied by the large PR in Fig. 1(c). The vibration patterns of Yb and La atoms in skutterudites are analog to the resonant modes proposed by the previous theoretical studies [32–35], where the contributions of guest atoms dominate in a certain frequency range.

Phonon lifetimes displayed in Figs. 1(d)–1(f) are calculated for both filler-dominant modes and framework-dominant lattice phonons under three-phonon process. In these filled skutterudites, the lifetimes of framework-dominant modes have few differences and agree with the ω^{-2} relationship of the umklapp process especially in the low-frequency parts. Comparing with lifetimes of Co_4Sb_{12} (see the Supplemental Material [24]), those for the framework in filled systems shift downwards. More importantly, filler-dominant modes, especially Yb-dominant modes, manifest more greatly suppressed lifetimes than those of framework part, i.e., umklapp process, shown in Fig. 1(d). It indicates that the localized Yb modes evoke strong phonon scattering.

In order to find the origin of this abnormal scattering, we investigate the scattering channels and the strength of their three-phonon interactions. The comparison of JDOS of filled skutterudites and Co_4Sb_{12} is given in the Supplemental Material [24]. It is clear that the small increase of JDOS in filled systems is not sufficient to make the strong scattering. Equation (2) shows that the scattering matrix element $\Phi_{\lambda\lambda'\lambda''}$ plays a significant role in the phonon lifetimes [36,37]. In the avoided crossing region [10,11,15], the interactions between the filler and the framework modes are apparently stronger than other parts due to the hybridization of these two kinds of vibrations. Therefore, we choose two modes λ_1, λ_2 in the avoided crossing region along the Γ-P direction with frequencies, 0.94 and 1.20 THz, approaching Yb-dominant frequencies and the $\boldsymbol{q}_1$ point (0.108, 0.108, 0.108) as shown in the Supplemental Material [24]. Their three-phonon interactions strength $|\Phi_{\lambda\lambda'\lambda''}|^2$ are calculated and depicted in Figs. 2(a) and 2(b), respectively.

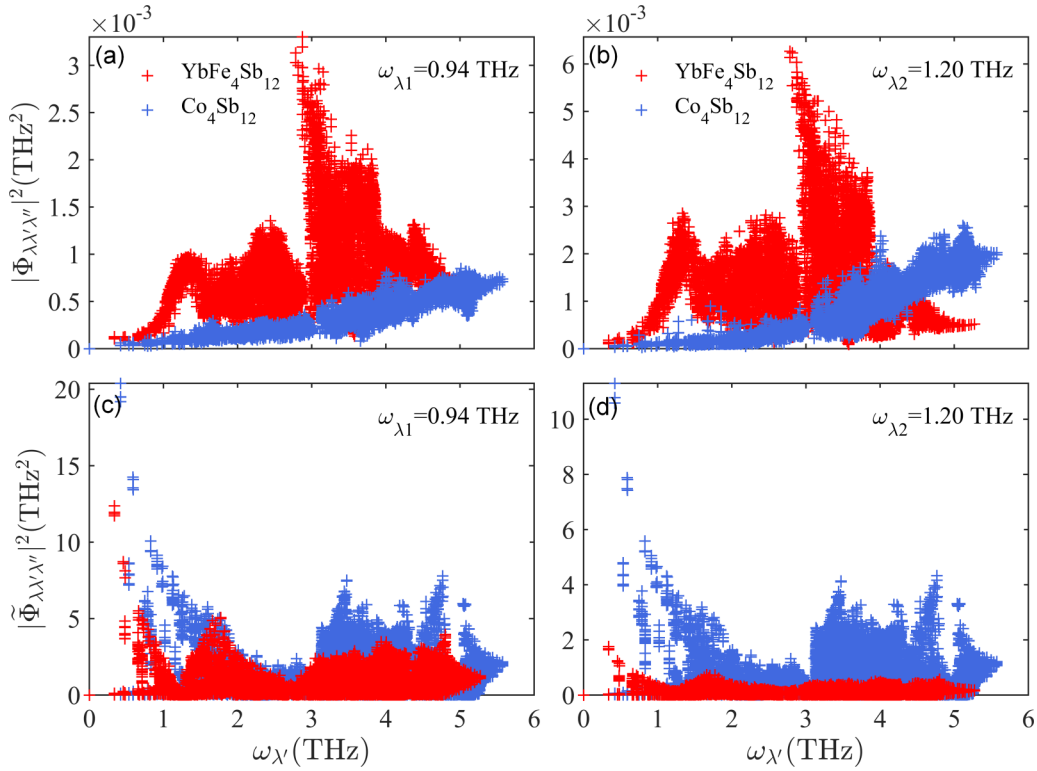

FIG. 2. (a,b) Calculated strength of three-phonon interactions $|\Phi_{\lambda\lambda'\lambda''}|^2$ of λ_1 and λ_2 modes in $YbFe_4Sb_{12}$ (red) and Co_4Sb_{12} (blue) at $\boldsymbol{q}_1 = (0.108, 0.108, 0.108)$ along the Γ-P direction (see Fig. S1 in the Supplemental Material [24]). For a comparison, recalculated $|\tilde{\Phi}_{\lambda\lambda'\lambda''}|^2$ ignoring the directions of atomic eigenvectors are also illustrated in (c,d). The frequencies of λ_1 and λ_2 modes in $YbFe_4Sb_{12}$ are indicated in the diagrams.

Comparing with Co_4Sb_{12}, the scattering matrix elements of $YbFe_4Sb_{12}$ are prominently increased at the broad-frequency range 1.0–4.0 THz. These higher scattering strengths are ascribed to the participations of Yb in the three-phonon process by both hybridized and single modes. Namely, the anharmonic interactions between Yb and framework vibrations are very strong. For comparison, we recalculate the scattering matrix element $\tilde{\Phi}_{\lambda\lambda'\lambda''}$ by replacing eigenvectors $e^{\lambda}_{\alpha i}$ with their absolute length $|e^{\lambda}_{\alpha i}|$ in Eq. (1), i.e., ignoring the vibration directions. As seen in Figs. 2(c) and 2(d), anharmonicities of λ_1, λ_2 modes in $YbFe_4Sb_{12}$ are not increased in this scenario comparing with those of Co_4Sb_{12}. When the hybridization of Yb increases, anharmonicities of the λ_2 mode are much smaller than those of Co_4Sb_{12}. Therefore, we infer that the alignment extent of the eigenvectors for Yb and the framework atoms is considerably higher than that of Co_4Sb_{12}, which eventually greatly increases the strength of three-phonon interactions in $YbFe_4Sb_{12}$. Additionally, the strengths of anharmonic scattering of $LaFe_4Sb_{12}$ and $BaFe_4Sb_{12}$ are also calculated and shown in the Supplemental Material [24]. Both of these results show the guest-host coupling behavior suggested by the synergistic vibrations between fillers and the framework. It differs from the traditional way by enhancing the anharmonic IFCs for stronger scattering strengths.

In spite of the coupling characteristic, the phonon lifetimes of $LaFe_4Sb_{12}$ and $BaFe_4Sb_{12}$ do not show similar abnormal scatterings, though the PR of La- and Yb-dominant modes are similar. We exchange the harmonic or anharmonic IFCs of $YbFe_4Sb_{12}$ and $LaFe_4Sb_{12}$, and recalculate the lifetimes of $LaFe_4Sb_{12}$. In Fig. 3(a), the lifetimes of $LaFe_4Sb_{12}$ with the harmonic IFC from $YbFe_4Sb_{12}$ are very close to those of $YbFe_4Sb_{12}$, while results of the changed anharmonic IFC do not alter much compared with the original lifetimes. This proves that the harmonic IFC is decisive in the strong scattering by filler vibrations. Two important factors relating the harmonic IFC with the anharmonic scattering are the scattering channels and the eigenvectors, respectively. In Fig. 3(b), we compare the JDOS before and after changing the harmonic IFC, and find there is little difference made by this substitution. As for the eigenvectors, we investigate the atomic displacement parameters (ADPs) which are proportional to the length of the atomic eigenvectors shown by Eq. (9) [38]. In Fig. 3(c), the ADPs of Yb are much larger than those of both La and Ba, indicating the eigenvectors of Yb possess the longer length. These systematic analyses under the perturbation theory help us come to the conclusion that the localized vibrations of fillers with large amplitudes do couple with neighboring Sb atoms leading to the abnormally strong scattering of the filler-dominant modes eventually.

$$\left\langle \left| \boldsymbol{u}_i^{\alpha} \right|^2 \right\rangle = \frac{\hbar}{2NM_i} \sum_{\lambda} \frac{1 + 2\boldsymbol{n}_{\lambda}}{\boldsymbol{\omega}_{\lambda}} \left| \boldsymbol{e}_{i\alpha}^{\lambda} \right|^2. \tag{9}$$

B. The role of resonant scattering on κ_L

However, we could not appropriately describe the scattering mechanism of these filler vibrations by the paradigm of the three-phonon process. Figure 4 displays the theoretical κ_Ls of these filled skutterudites calculated with temperature-

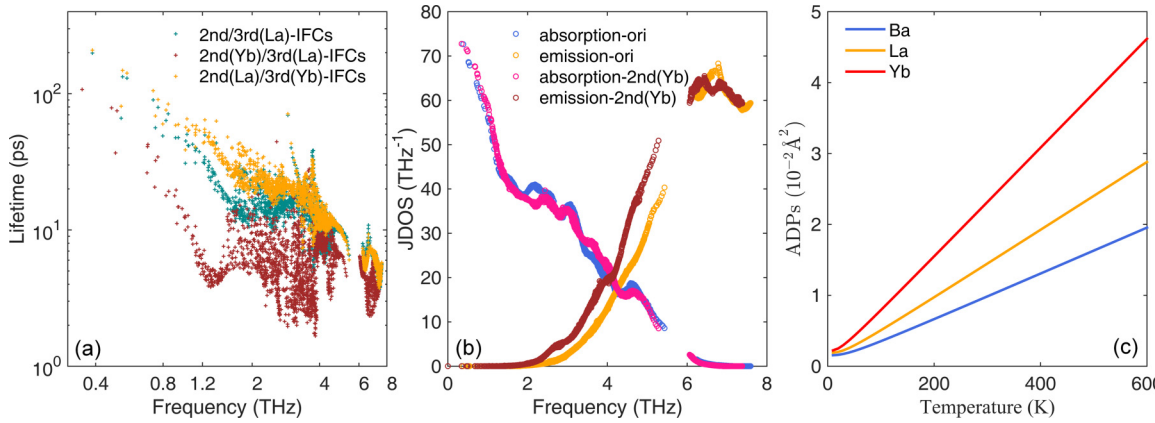

FIG. 3. Recalculated phonon transport properties of $LaFe_4Sb_{12}$ after exchanging IFCs by those of $YbFe_4Sb_{12}$. (a) Lifetimes obtained by harmonic or anharmonic IFCs of $YbFe_4Sb_{12}$, respectively. (b) JDOS before and after substituting the harmonic IFC of $YbFe_4Sb_{12}$. (c) Atomic displacement parameters (ADPs) of fillers Yb, La, and Ba in filled skutterudites.

dependent IFCs by the same approaches used in our recent work [17]. Considerations on the temperature effects on IFCs do alter the temperature dependence of $\kappa_L \sim T^{-0.5}$. Comparing with the traditional T^{-1} relationship gotten from anharmonic scattering [15], this is an important improvement towards the experimental κ_L of filled skutterudites [16]; but the obvious difference between values of theoretical and experimental κ_L implies the three-phonon process underestimates the scattering of filler vibrations. To diminish these discrepancies, resonant scattering beyond the three-phonon process must be introduced for the filler-dominant modes as described in Eq. (10). In this way, the recalculated κ_Ls could be in good agreement with the experimental data as shown in Fig. 4. Aiming at assessing the role of the resonant scattering, we depict the lifetimes of filler-dominant modes modified by $\tau_R^{-1} = C^*\omega^2/[(\omega_0^2 - \omega^2)^2 + \Delta^2]$ [33] in Fig. 5. They are more than two orders lower than the lifetimes of framework modes obtained by anharmonic scattering. It not only proves the importance of introducing the resonant scattering, but also illustrates the accurate impact of filler vibrations on the phonon transport. In a word, the filler-dominant modes nearly eliminate the lattice phonon with the same frequencies from the heat transportation and cause huge thermal resistance.

$$\kappa_L = \frac{1}{NV}\left[\sum_{\lambda \notin filler} C_\lambda v_\lambda^2 \tau_\lambda + \sum_{\lambda \in filler} C_\lambda v_\lambda^2 \tau_R\right]. \quad (10)$$

C. Dynamic process of resonant scattering

Given the significant effects of the resonant phonon scattering on the ultralow κ_L in the filled skutterudites, it is thus interesting to explore its physical origin. We examine the transient features of the filler vibrations through the wavelet analysis on MD trajectories. This perspective is analog to the hypothesis from the INS study on the dynamic behavior of $EuFe_4Sb_{12}$ [6]. Figure 6(a) shows the static power spectra of Yb and depicts its vibration-frequency range 0.9–1.4 THz. Figure 6(b) shows the time-frequency power spectrum of Yb.

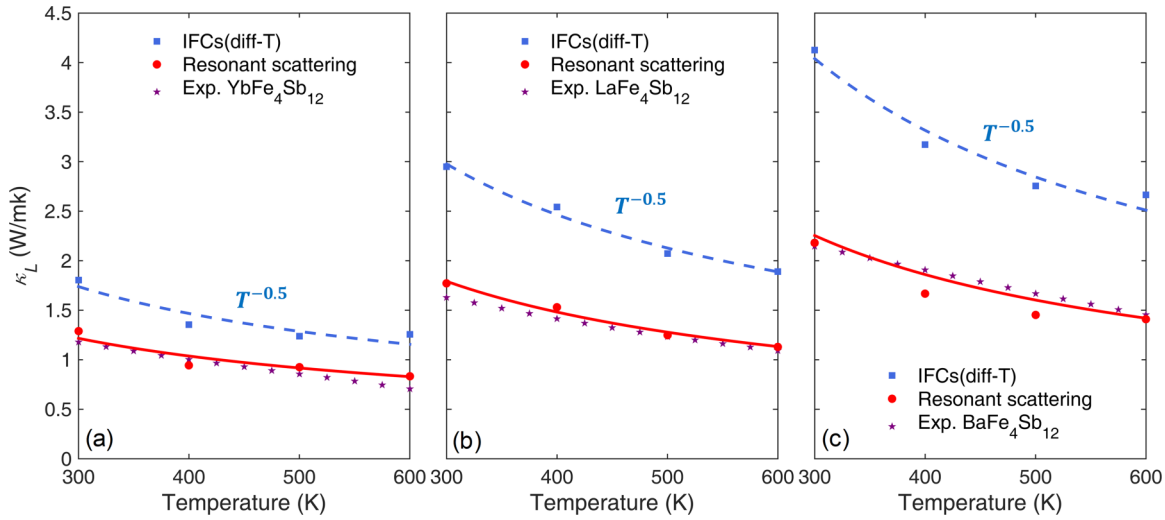

FIG. 4. Calculated lattice thermal conductivity κ_L of filled skutterudites, (a) $YbFe_4Sb_{12}$ [17], (b) $LaFe_4Sb_{12}$, and (c) $BaFe_4Sb_{12}$, by TDEP (blue squares). Recalculated κ_L by an additional resonant scattering mechanism are also depicted by red circles. Dashed and solid lines are obtained by fitting the blue and red symbols, respectively. Purple stars are experimental data taken from Ref. [16].

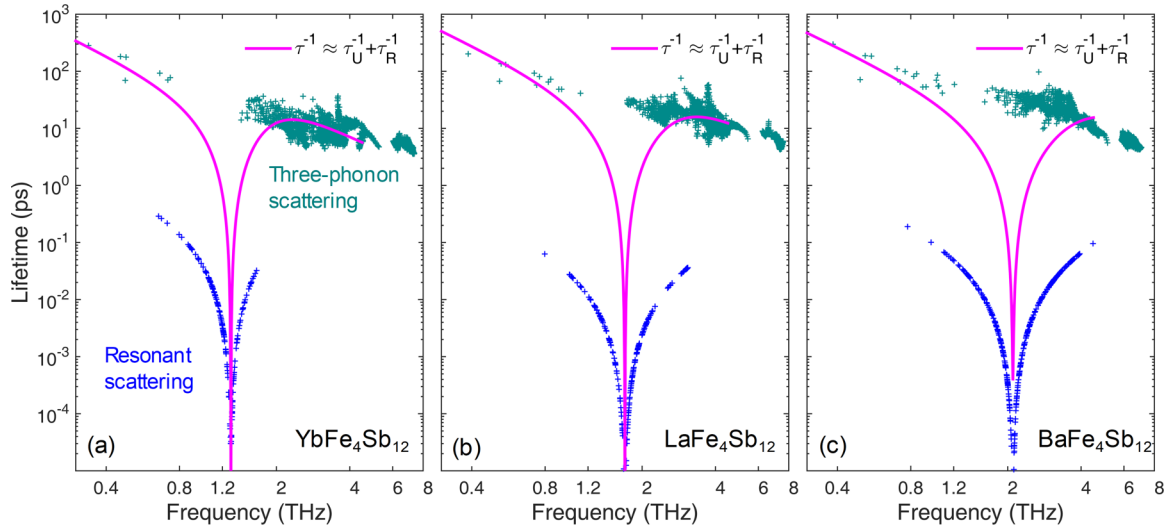

FIG. 5. Recalculated lifetimes of (a) $YbFe_4Sb_{12}$, (b) $LaFe_4Sb_{12}$, and (c) $BaFe_4Sb_{12}$ by modifying filler modes with resonant scattering. Blue and cyan parts are filler- and framework-dominant modes, respectively. The pink curves are fitting lines by the relation $\tau^{-1} \approx \tau_U^{-1} + \tau_R^{-1}$.

It maps the power intensity at each time step and frequency via a contour plot. The peak frequencies at different times are also drawn by the solid line. We define the Yb vibration with lower frequency around 1.0 THz as the the ground state, and higher frequency around 1.4 THz as the excited state. Interestingly, the Yb vibration is fluctuating between the ground state and the excited state, both of which emerge alternately in the time domain. The fluctuated frequencies of Yb indicate energy transferring between Yb and the framework; i.e., some lattice phonons would be absorbed (absorption process) in one time period, and be emitted (emission process) at a later time. Moreover, the time durations of the absorption and emission processes are about 5 ps, comparable to lifetimes of lattice phonons approaching Yb frequencies shown in Fig. 1(d). These phonons do contribute less to the heat current due to being trapped during the relatively long absorption and emission processes [34,35]. This dynamic process describes how the Yb vibration keeps lattice phonons from propagating in the thermal transport through the resonant scattering. As a reference, we also plot the time-frequency power spectra of La and Ba in the Supplemental Material [24].

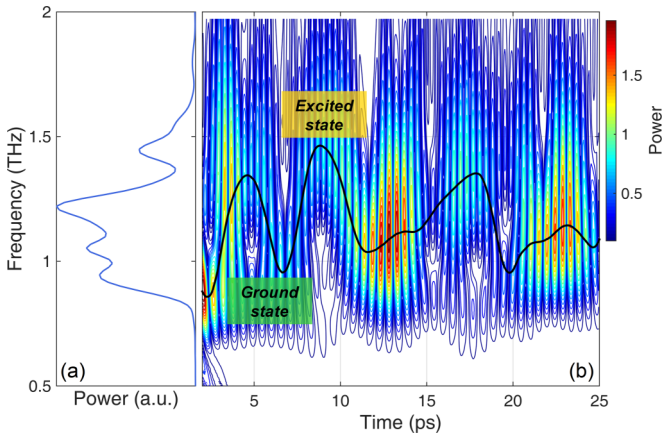

FIG. 6. (a) The statistical power spectra of Yb at 300 K in filled skutterudite calculated by the Fourier transform. (b) Time-frequency power spectra of the Yb obtained by the wavelet transform. The colors in this contour plot represent the power intensity at each time and frequency. The frequencies for the peak power intensities at different time steps are depicted by the solid line.

The fluctuation of Yb vibration is subjected to the interactions between Yb and the framework. We investigate the correlation properties of Yb and neighboring Sb in the dynamic process to probe their interactions. Therefore, the time-frequency coherence is obtained by applying the wavelet transform on the VCF. Figure S11 (see the Supplemental Material [24]) illustrates the time-evolution correlation properties between Yb and neighboring Sb at the frequency range 1.0–1.4 THz. Then, we get slices of the time-dependent coherence at 1.0 and 1.4 THz shown in Fig. 7(a), for the better illustration of the variance of Yb-Sb correlations in the time domain. We find the coherence of Yb-Sb is 0.7 at the ground state and gradually reduces to 0.1 at the excited state [Fig. 6(b)]. The changing correlations must reflect the different atomic configurations during different states. In Fig. 7(b), we show the radial distribution functions (RDFs) of Yb, with zero distance representing the Yb-Sb bond lengths at their equilibria. During the ground states, the RDF of Yb is 0.1 Å smaller than the equilibrium Yb-Sb bond length, indicating that Yb statistically gets close to the neighboring Sb. On the other hand, Yb stays on the center of the cage during the excited state. Since the Yb and Sb atoms are relatively closer at the ground state, they can form a weak dipole pair, which enhances the correlations. The dipole pair also causes a heavier oscillator, thus the lower vibrational frequency (1.0 THz at the ground state). Due to the cagelike structure, the interaction between Yb and the framework is restricted to the neighboring Sb atoms, other than the whole lattice. At the excited state, Yb vibrates independently, and the frequency is then enhanced. Yb atoms switch between the two states, absorbing and emitting lattice phonons, in a period of 5 ps, which can be phenomenologically treated as the resonant scattering mechanism. Therefore, we have provided the real-space picture for the physical processes of the resonant

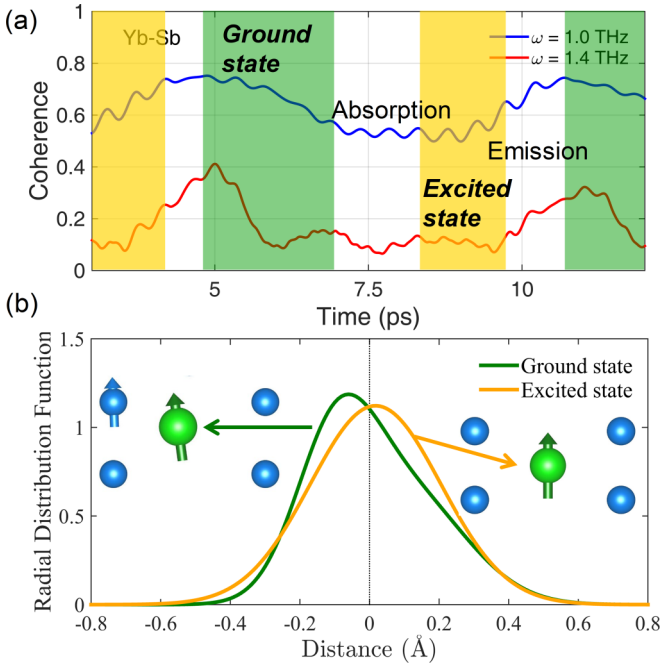

FIG. 7. (a) The velocities coherence of Yb-Sb versus time at the ground state and the excited state. The locations at time axis for these two states are determined from the time-frequency power spectrum depicted in Fig. 6(b). (b) The radial distribution functions of Yb-Sb at the ground and excited states. The cage radius of $YbFe_4Sb_{12}$ at the equilibrium (3.42 Å) is set as the reference distance.

scattering in filled skutterudites. In addition, the correlations between different Yb atoms are calculated and shown in the Supplemental Material [24]. The coherence of the Yb pair is low (0.05–0.18), indicating the insignificant role of the Yb pair in the Yb vibrations.

IV. CONCLUSIONS

In summary, we apply AIMD to simulate the dynamic process of three fully filled skutterudites $YbFe_4Sb_{12}$, $LaFe_4Sb_{12}$, and $BaFe_4Sb_{12}$. The TDEP method is employed to calculate their finite-temperature lattice dynamics and phonon transport properties. The quasilocalized filler vibrations with large amplitudes are found to be the reason for the scattering being abnormally stronger than the umklapp process, especially in $YbFe_4Sb_{12}$. But the calculated κ_Ls under the umklapp process solely are higher than the experimental results. The introduction of resonant scattering for filler-dominant modes accurately describes the ultralow κ_Ls of filled skutterudites by strongly eliminating low-frequency lattice phonons from heat currents. To investigate its origin, the dynamic process of the resonant scattering is found through the wavelet analysis applied on velocity correlation functions. The Yb atom correlates with neighboring Sb notably at the ground vibration state while it vibrates independently at the excited state. The fluctuated interactions between Yb and the neighboring framework trap lattice phonons between the absorption and emission processes of the Yb vibration with a time period of 5 ps. It strongly hinders the propagations of low-frequency lattice phonons. Thus, we demonstrate the physical picture of resonant scattering and explain how the harmonic and localized Einstein oscillators of fillers significantly suppress the κ_Ls of filled skutterudites. Understanding the role of fillers played in the thermal transport renews our recognitions of the lattice dynamics and phonon propagations at the microscopic level in these thermoelectric materials with chemical bond hierarchies.

ACKNOWLEDGMENTS

This work is supported by the National Key Research and Development Program of China (Grant No. 2017YFB0701600), the National Natural Science Foundation of China (Grants No. 51632005, No. 51572167, No. 11574333, and No. 11674211) and the Program of Shanghai Subject Chief Scientist (Grant No. 16XD1401100). W.Z. acknowledges the support from Guangdong Innovation Research Team Project (Grant No. 2017ZT07C062) and Shenzhen Pengcheng-Scholarship program, and the fruitful discussion with Dr. Brian C. Sales from Oak Ridge National Laboratory. J.Y. acknowledges the supports from the Program for Professor of Special Appointment (Eastern Scholar) at Shanghai Institutions of Higher Learning (No. TP2015041) and 111 Project (No. D16002).

[1] G. S. Nolas, D. T. Morelli, and T. M. Tritt, Annu. Rev. Mater. Sci. **29**, 89 (1999).
[2] X. Shi, S. Bai, L. Xi, J. Yang, W. Zhang, L. Chen, and J. Yang, J. Mater. Res. **26**, 1745 (2011).
[3] M. Rull-Bravo, A. Moure, J. F. Fernández, and M. Martín-González, RSC Adv. **5**, 41653 (2015).
[4] B. C. Sales, D. Mandrus, B. C. Chakoumakos, V. Keppens, and J. R. Thompson, Phys. Rev. B **56**, 15081 (1997).
[5] X. Shi, J. Yang, J. R. Salvador, M. Chi, J. Y. Cho, H. Wang, S. Bai, J. Yang, W. Zhang, and L. Chen, J. Am. Chem. Soc. **133**, 7837 (2011).
[6] G. J. Long, R. P. Hermann, F. Grandjean, E. E. Alp, W. Sturhahn, C. E. Johnson, D. E. Brown, O. Leupold, and R. Ruffer, Phys. Rev. B **71**, 140302 (2005).
[7] R. P. Hermann, R. Jin, W. Schweika, F. Grandjean, D. Mandrus, B. C. Sales, and G. J. Long, Phys. Rev. Lett. **90**, 135505 (2003).
[8] Y. Wang, X. Xu, and J. Yang, Phys. Rev. Lett. **102**, 175508 (2009).
[9] I. K. Dimitrov, M. E. Manley, S. M. Shapiro, J. Yang, W. Zhang, L. D. Chen, Q. Jie, G. Ehlers, A. Podlesnyak, J. Camacho, and Q. Li, Phys. Rev. B **82**, 174301 (2010).
[10] C. H. Lee, I. Hase, H. Sugawara, H. Yoshizawa, and H. Sato, J. Phys. Soc. Jpn. **75**, 123602 (2006).
[11] M. Christensen, A. B. Abrahamsen, N. B. Christensen, F. Juranyi, N. H. Andersen, K. Lefmann, J. Andreasson, C. R. Bahl, and B. B. Iversen, Nat. Mater. **7**, 811 (2008).
[12] E. S. Toberer, A. Zevalkink, and G. J. Snyder, J. Mater. Chem. **21**, 15843 (2011).

[13] M. M. Koza, M. R. Johnson, R. Viennois, H. Mutka, L. Girard, and D. Ravot, Nat. Mater. **7**, 805 (2008).
[14] H. Euchner, S. Pailhès, L. T. K. Nguyen, W. Assmus, F. Ritter, A. Haghighirad, Y. Grin, S. Paschen, and M. de Boissieu, Phys. Rev. B **86**, 224303 (2012).
[15] W. Li and N. Mingo, Phys. Rev. B **91**, 144304 (2015).
[16] P. F. Qiu, J. Yang, R. H. Liu, X. Shi, X. Y. Huang, G. J. Snyder, W. Zhang, and L. D. Chen, J. Appl. Phys. **109**, 063713 (2011).
[17] Y. Wang, W. Qiu, H. Yang, L. Xi, J. Yang, and W. Zhang, Acta Phys. Sin. **67**, 016301 (2018).
[18] O. Hellman, I. A. Abrikosov, and S. I. Simak, Phys. Rev. B **84**, 180301 (2011).
[19] O. Hellman and I. A. Abrikosov, Phys. Rev. B **88**, 144301 (2013).
[20] A. Togo, F. Oba, and I. Tanaka, Phys. Rev. B **78**, 134106 (2008).
[21] G. Kresse and J. Furthmüller, Phys. Rev. B **54**, 11169 (1996).
[22] P. E. Blöchl, Phys. Rev. B **50**, 17953 (1994).
[23] J. P. Perdew, K. Burke, and M. Ernzerhof, Phys. Rev. Lett. **77**, 3865 (1996).
[24] See Supplemental Material at http://link.aps.org/supplemental/10.1103/PhysRevB.98.054304 for details of computational conditions, results of temperature-dependent phonon interactions evaluated by TDEP, and illustrations of the time-frequency power spectrum by wavelet analysis.
[25] R. A. Cowley, Rep. Prog. Phys. **31**, 123 (1968).
[26] M. P. Allen and D. J. Tildesley, *Computer Simulation of Liquids* (Oxford University Press, Oxford, 1989).
[27] M. B. Ruskai, G. Beylkin, and R. Coifman, *Wavelets and their Applications* (Jones and Bartlett, Boston, 1992).
[28] M. Pagliai, F. Muniz-Miranda, G. Cardini, R. Righini, and V. Schettino, J. Mol. Struct. **993**, 438 (2011).
[29] A. Rahman, Phys. Rev. **136**, A405 (1964).
[30] K. Shin and J. Hammond, *Fundamentals of Signal Processing for Sound and Vibration Engineers* (John Wiley & Sons, Berlin, 2008).
[31] S. Pailhes, H. Euchner, V. M. Giordano, R. Debord, A. Assy, S. Gomes, A. Bosak, D. Machon, S. Paschen, and M. de Boissieu, Phys. Rev. Lett. **113**, 025506 (2014).
[32] D. K. Brice, Phys. Rev. **140**, A1211 (1965).
[33] R. O. Pohl, Phys. Rev. Lett. **8**, 481 (1962).
[34] M. Wagner, Phys. Rev. **131**, 1443 (1963).
[35] C. T. Walker and R. O. Pohl, Phys. Rev. **131**, 1433 (1963).
[36] D. A. Broido, M. Malorny, G. Birner, N. Mingo, and D. A. Stewart, Appl. Phys. Lett. **91**, 231922 (2007).
[37] T. Tadano, Y. Gohda, and S. Tsuneyuki, Phys. Rev. Lett. **114**, 095501 (2015).
[38] A. Togo and I. Tanaka, Scr. Mater. **108**, 1 (2015).